

Probing Gluons in Nuclei: the Case of η'

Jamal Jalilian-Marian¹ and Sangyong Jeon^{2,3}

¹*Physics Department, BNL, Upton, NY 11973, USA*

²*Department of Physics, McGill University, Montreal, QC H3A-2T8, Canada*

and

³*RIKEN-BNL Research Center, BNL, Upton, NY 11973, USA*

November 29, 2001

Abstract

Using the recently proposed $gg\eta'$ effective vertex, we investigate the production of η' from gluon fusion in pA collisions. We show that measuring η' production cross-section at moderate $x_{\eta'}$ yields direct information on the small x gluon distribution function of the nucleus. At RHIC, the smallest accessible x turns out to be $O(10^{-5})$ and at LHC, it is $O(10^{-8})$. Therefore, η' is an excellent probe of the Color Glass Condensate.

1 Introduction

The η' meson has many interesting properties, the most discussed being its unusual mass. By spontaneously breaking $U(3)$ symmetry of the hadronic Lagrangian, one would expect that η' would be a Goldstone boson whose finite mass is due to the finite mass of the quarks. In reality, the η' mass ($M = 0.958 \text{ GeV}$) is much heavier than the mass of the η ($M_\eta = 0.547 \text{ GeV}$). The quark model Gell-Mann-Okubo formula for the singlet and the octet mass

$$M_0^2 = \frac{f_\pi^2}{3f_0^2} (m_{K^+}^2 + m_{K^0}^2 + m_{\pi^+}^2) \quad (1)$$

and

$$M_8^2 = \frac{1}{3} (2m_{K^+}^2 + 2m_{K^0}^2 + 2m_{\pi^+}^2 + m_{\pi^0}^2) \quad (2)$$

is incapable of explaining this large mass difference between the (mostly) flavor octet state η and the (mostly) singlet state η' . In fact, the singlet mass M_0 is smaller than the octet mass M_8 . Therefore, in the zero quark mass limit, about half of the η' mass remains while the octet pseudo-scalar meson (π, K, η) masses go to zero.

The resolution of this $U_A(1)$ problem was provided by 't Hooft [1] and Witten [2]. In these works, it was argued that the anomalously large mass of η' is due to the mixing of the gluon state with the flavor-singlet quark state through the axial anomaly

$$\partial^\mu J_\mu^5 = 2i \sum_f m_f \bar{q}_f \gamma_5 q_f + 2N_f \frac{g^2}{16\pi^2} \text{Tr} (G_{\mu\nu} \tilde{G}^{\mu\nu}) \quad (3)$$

with non-vanishing $\langle G\tilde{G} \rangle$. This implies that the η' mesons have a large glue content. It also implies that the gluon fusion process $gg \rightarrow \eta'$ is possible.

In this paper, we study the generation of η' mesons from such a gluon fusion process in proton-nucleus ' pA ' collisions. In particular, we argue that measuring the η' meson momentum spectrum enables us to have a direct access to the gluon density in the small x region of the heavy nucleus. This is made possible by using a recently proposed effective vertex by Atwood and Soni [3] between gluons and the η' meson.

In [3], as a step to explain an anomalously large B to η' branching fraction, the authors wrote down a Wess-Zumino-Witten type of effective vertex:

$$T_{\lambda\gamma} \delta^{ab} = H(p^2, q^2, P^2) \delta^{ab} \epsilon_{\mu\nu\alpha\beta} p^\mu q^\nu (\epsilon_p^\alpha)_\lambda (\epsilon_q^\beta)_\gamma \quad (4)$$

roughly corresponding to an interaction Lagrangian of the form $\mathcal{L} \sim \eta' G \tilde{G}$. Here, p, q are the gluons momenta, $\epsilon_{p,q}^{\alpha,\beta}$ are the associated polarization vectors, and the δ^{ab} denotes the singlet combination of the gluons. From now on, we denote the η' momentum by a capital letter P . The factor $H(p^2, q^2, P^2)$ is a form factor. By analyzing $J/\psi \rightarrow \eta' \gamma$ process, the authors of [3] then estimate that in the on-shell limit

$$H_0 \equiv H(0, 0, M^2) \approx 1.8 \text{ GeV}^{-1} \quad (5)$$

where $M = 0.958 \text{ GeV}$ is the mass of the η' meson. This vertex was then used to analyze the B -boson decay to η' assuming that the p^2 and q^2 dependence of H is weak¹. This form of effective vertex has been also confirmed by a calculation of the triangle diagram contribution to the axial anomaly [5].

The above effective vertex represents a *hadronization matrix element* between a two-gluon state and a hadron state. To the authors' knowledge, this is unique. Certainly, many constituent quark models can relate valence quarks to hadrons. However, except for the above $gg\eta'$ effective vertex, there is no other known matrix element between the gluons and a known hadron state. We also note that the momenta involved in this process is not so soft compared to Λ_{QCD} or the pion mass since the η' mass is almost 1 GeV.

Recently, these interesting features of the $gg\eta'$ vertex were exploited to calculate the η' production from a hadronizing quark-gluon plasma [6]. In that study, a Boltzmann equation was used to evolve the η' density towards the hadronization time in heavy ion collisions. To use the $gg\eta'$ vertex in this 'AA' environment, a certain set of assumptions had to be made. These assumptions mainly involve the as-yet-unknown in-medium properties of the particles and vertices involved in the calculation.

In this paper, we focus on production of η' in pA collisions for two reasons. First, much is known about the structure of proton from DIS experiments at HERA and elsewhere [7]. Assuming that we understand the parton distributions in a proton, pA experiments are an excellent tool with which to investigate parton distributions of nuclei at small x . This becomes even more important in light of the fact that not much is known about modification of parton distributions in nuclei at small

¹This weak dependence assumption has been questioned by Kagan and Petrov [4] who argued that when one of the gluon momenta is off-shell, the form factor has to be replaced by

$$H(q^2, p^2, M^2) \approx H_0 M^2 / (M^2 - q^2). \quad (6)$$

However, this is not relevant to the present study.

x and intermediate Q^2 since all existing fixed target eA experiments have limited coverage in x and Q^2 [8, 9, 10, 11, 12]. This region of small x and intermediate Q^2 ($\sim 1 - 10 \text{ GeV}^2$) is the domain of high gluon density QCD and semi-hard physics where interesting phenomena such as saturation of gluons, etc. are expected to occur. pA experiments will give us a new venue, in addition to eA and AA , in which to investigate the high gluon density phase of QCD.

Also, pA collisions are much cleaner than AA in the sense that one can avoid many of the complications due to the in-medium effects. We do not expect to have a Quark Gluon Plasma (or a hot hadronic phase) created in pA collisions and can therefore avoid the difficulties associated with understanding the possible formation of plasma and its detailed properties. In this work, we will show how one can extract the nuclear gluon distribution function at small x from pA experiments at RHIC assuming one knows the gluon distribution function in a proton at not too small values ($O(x \sim 0.1 - 0.01)$).

It should be noted that even though our experimental knowledge of the parton distribution functions in a proton is good, due mostly to HERA, in some pp induced processes such as $pp \rightarrow \gamma X$ or $pp \rightarrow \pi X$, it is quite common to introduce an “intrinsic” momentum $\langle k_t^2 \rangle$ into the standard parton distribution functions in order to fit the experimental data [13]. For example,

$$xG(x, Q^2) = \int d^2k_t xG(x, Q^2, k_t^2) \equiv \int d^2k_t xG(x, Q^2) f(k_t^2) \quad (7)$$

where $f(k_t^2)$ is usually taken to be a Gaussian with width $\langle k_t^2 \rangle$. More explicitly,

$$f(k_t^2) = \frac{1}{\pi \langle k_t^2 \rangle} \exp \left(-\frac{k_t^2}{\langle k_t^2 \rangle} \right) \quad (8)$$

so that $\int d^2k_t f(k_t^2) = 1$. The value of $\langle k_t^2 \rangle$ is extracted from best fits to experimental data on dileptons, dijets, etc. and can be as large as $1 - 5 \text{ GeV}^2$ at the Tevatron. Its value depends also on the energy of the collision and the process considered and is expected to be smaller for production of heavier particles.

The origin of this “intrinsic momentum” is mostly initial state radiation of soft gluons. A rigorous investigation of these soft emissions has been carried out in some processes, such as dilepton production, which effectively introduces this “intrinsic” momentum into the standard collinear factorization based cross sections [14]. In addition to the “intrinsic” momentum due to the initial state radiation, there is a genuine non-perturbative contribution which is energy and process independent and is of order $O(200 - 300 \text{ MeV})$ consistent with the uncertainty principle. Phenomenologically, these results can also be obtained by using the modified parton distribution

functions as defined in (7) without the resummation of the soft gluon radiation. This is especially useful since this soft gluon resummation has been carried out only for a limited number of processes. Nevertheless, this resummation is usually taken to be the theoretical justification for introduction of this “intrinsic” momentum into the standard parton distribution functions. There is also the Cronin effect in pA collisions which can contribute to this intrinsic momentum. Even though Cronin effect is not well understood in pQCD, one can phenomenologically understand it in terms of multiple scattering of the proton on the nucleus which causes the p_t broadening of the proton [15].

In large nuclei and at small x , one also has to include high gluon density effects. In [16, 17, 18, 19, 20] it is shown that high gluon densities lead to a potentially large intrinsic scale $Q_s^2(x) \sim A^{1/3} \frac{1}{x^{2-4}}$ in large nuclei. Most gluons in the wave function of a nucleus in a high energy collision have momenta of the order of this scale. In this paper we will investigate production of η' in pA collisions as means of extracting the gluon distribution function of nuclei at small x and study its dependence on the intrinsic momentum $\langle k_t^2 \rangle$ in protons and on saturation scale $Q_s^2(x)$ in nuclei.

2 η' Production Cross Section

In this section, we will calculate the η' production in pA collisions and show how to extract the gluon distribution function of the nucleus A . We will consider three distinct cases; first, we will calculate the η' production cross section, with the standard gluon distribution function, and using the collinear factorization formalism. Then, we will consider the case when the gluons in the nucleus A are at small x and include saturation effects in the nuclear gluon distribution function. Finally, we will allow for “intrinsic” momentum in a proton and consider the case when the gluon distribution function of the proton is also modified to take the “intrinsic” momentum of the proton into account.

2.1 Collinear Factorized Cross Section

Using collinear factorization theorems in perturbative QCD, one can write the η' production cross section in pA collisions as

$$d\sigma^{pA \rightarrow \eta' X} = \int dx_1 dx_2 G^p(x_1, Q_f^2) G^A(x_2, Q_f^2) d\sigma^{gg \rightarrow \eta'} \quad (9)$$

where $G(x_1, Q_f^2)$, $G(x_2, Q_f^2)$ are the gluon distribution function of the proton and nucleus respectively and x_1 and x_2 are the momentum fraction of the incoming

gluons while $x_L = 2P_z/\sqrt{s}$ and $x_E = 2E_P/\sqrt{s}$ are the momentum and energy fractions of the produced η' respectively. The distribution functions, $G(x_1, Q_f^2)$ and $G(x_2, Q_f^2)$, depend on a factorization scale Q_f^2 which is shown explicitly and will be taken to be $\sim M_{\eta'}^2$ in numerical calculations. We also note that there are no intrinsic momenta included in either distribution functions since it is not, strictly speaking, allowed in collinear factorization formalism.

The partonic cross-section for $gg \rightarrow \eta'$ is given by

$$d\sigma^{gg \rightarrow \eta'} = \frac{1}{4\sqrt{(p \cdot q)^2}} \frac{d^3P}{(2\pi)^3 2E_P} |T_{gg \rightarrow \eta'}|^2 (2\pi)^4 \delta^4(P - p - q) \quad (10)$$

where p and q are the momenta of the incoming gluons while P is the momentum of the produced η' . The matrix element squared, after averaging over the initial spin and color degrees of freedom, becomes

$$|T_{gg \rightarrow \eta'}|^2 = \frac{1}{64} H_0^2 M_{\eta'}^4 \quad (11)$$

Using (11), the differential cross section becomes

$$d\sigma^{gg \rightarrow \eta'} = \frac{H_0^2 M_{\eta'}^2}{128} \frac{d^3P}{(2\pi)^3 2E_P} (2\pi)^4 \delta^4(P - p - q) \quad (12)$$

This is the elementary partonic cross section which goes into our calculation of η' production in pA collisions. It should be noted that collinear factorization for η' production has not been explicitly proven but is analogous to using (rigorously proven) collinear factorization in production of heavy quarks, high p_t jets, high mass dileptons, etc. and that since the natural scale involved (η' mass) is not very large, we may have large higher order corrections. This reflects itself in having cross sections which are quite sensitive to a change of factorization scale. Therefore, we feel our results are most reliable for the ratio of cross sections (pA over pp) rather than the absolute cross sections.

Using Eq. (12) and resolving the delta functions gives

$$\begin{aligned} \frac{d\sigma^{pA \rightarrow \eta' X}}{dx_L} &= \frac{\pi H_0^2 M_{\eta'}^2}{64 s x_E} G^p(x_+, Q_f^2) G^A(x_-, Q_f^2) \\ &= \frac{\pi H_0^2}{64 x_E} x_+ G^p(x_+, Q_f^2) x_- G^A(x_-, Q_f^2) \end{aligned} \quad (13)$$

where

$$x_{\pm} \equiv \frac{x_E \pm x_L}{2} = \frac{E_P \pm P_z}{\sqrt{s}} \quad (14)$$

In terms of the η' rapidity y or the longitudinal momentum fraction x_L , these are

$$x_{\pm} = \frac{M_{\eta'} e^{\pm y}}{\sqrt{s}} = \frac{\sqrt{x_L^2 + 4M_{\eta'}^2/s} \pm x_L}{2} \quad (15)$$

Here we take the positive y (as well as x_L) to correspond to the proton direction. For $x_L \gg M_{\eta'}/\sqrt{s}$, we can also write

$$x_+ \approx x_L \quad \text{and} \quad x_- \approx \frac{M_{\eta'}^2}{sx_L} \quad (16)$$

Equation (13) is a very simple and useful relation which enables us to extract the gluon distribution function of the nucleus *directly* (without any de-convolution, as is usually the case) from the experimentally measured η' production cross section. Here we are assuming that the gluon distribution function of a proton is known from HERA to good accuracy [21] (to better than 10%) which is the case unless $x_+ \gtrsim 0.2$. Also, in the region $x_+ \leq 10^{-4}$, one also has a large uncertainty in determining the gluon distribution function in a proton but we avoid this region by considering small values of x_- (recall x_- is the momentum fraction of gluons in the nucleus) since this is the region where nuclear modification of the gluon distribution function is most pronounced and least known.

Let us make a rough estimate of the x values one can probe in a high energy pA collision, such as those at RHIC or LHC. Since there are no experimental data on nuclear gluon distribution function at $x < 10^{-2}$ for $Q^2 > 1 \text{ GeV}$, we would like to focus on the small x (in the nucleus) kinematic region. This corresponds to the case when x_- in (13) is small. This in turn corresponds to the case when the measured η' has a large (much larger than its mass or P_t) longitudinal momentum, i.e. in the forward region (*c.f.* Eq.(15)).

At RHIC, the largest η' rapidity in the CM frame is about 5.36. Therefore in principle, the x_- range is

$$2.2 \times 10^{-5} < x_- < 0.005 \quad (17)$$

using Eq.(15). Since $x_+x_- = M^2/s$, this range of x_- corresponds to

$$0.0005 < x_+ < 1.0 \quad (18)$$

For instance, if we detect an η' at $y = 3.04$, that would correspond to $x_+ = 0.10$ and $x_- = 2.3 \times 10^{-4}$. At LHC, the largest η' rapidity in the CM frame is about 8.6. This implies that

$$3.2 \times 10^{-8} < x_- < 1.7 \times 10^{-4} \quad (19)$$

Since $x_+x_- = M^2/s$, this range of x_- corresponds to

$$1.7 \times 10^{-4} < x_+ < 1.0 \quad (20)$$

Again, if we fix $x_+ = 0.1$ or $y_{\eta'} = 6.35$, then $x_- = 3.0 \times 10^{-7}$. These would be, by orders of magnitude, the smallest values of x where gluon distribution in a nucleus has ever been measured. For example, the smallest values of x measurable in fixed target DIS experiments at CERN and Fermilab is $x \sim 10^{-2}$ at similar Q^2 [22, 23]. Therefore, by measuring the η' production cross section at large rapidities, one can, for the first time, determine the nuclear gluon distribution function at very small x and moderately large Q^2 . This will help one understand the nature of nuclear shadowing in QCD and determine the role of high parton density (higher twist) effects in nuclear shadowing.

2.2 Intrinsic Momenta

In this section, we will include the effects of intrinsic momenta in the gluon distribution of both proton and nucleus and investigate the dependence of η' production cross section on the intrinsic momenta. Since introducing the intrinsic momentum is done in the phenomenology spirit as discussed earlier, we will take its width to be the saturation scale, Q_s in nucleus. This comes about because at small values of x in nuclei, one encounters the high gluon density region of QCD where non-linear gluon recombination effects become important [25, 24, 26, 27, 28, 29]. The high gluon density introduces a new scale, the saturation scale $Q_s(x)$, which grows with energy ($Q_s^2(x) \gg \Lambda_{QCD}$ at small x) [30, 31, 32, 33, 34, 35, 36, 37, 38]. Most gluons in the wave function of a nucleus have momenta of the order of Q_s and therefore, one may take the average (the width of the Gaussian) intrinsic momentum to be this saturation scale Q_s . The value of Q_s^2 is estimated to be $\sim 1 - 2 \text{ GeV}^2$ at RHIC. As a first approximation and to keep our expressions simple, we will ignore the x dependence of Q_s^2 and calculate the η' production cross section with different values of Q_s .

As a first step, we will include the intrinsic momentum in a nucleus and not in a proton since the nuclear intrinsic momentum is expected to be much larger than that of a proton. Later, we will consider the most general case. The momenta of the incoming gluons are now, including the intrinsic momentum $p_t \sim Q_s$ in the nucleus,

$$q = (x_1\sqrt{s}/2, 0_t, x_1\sqrt{s}/2) \quad (21)$$

and

$$p = (x_2\sqrt{s}/2 + p_t^2/2x_2\sqrt{s}, p_t, -x_2\sqrt{s}/2 + p_t^2/2x_2\sqrt{s}) \quad (22)$$

The η' production cross section then becomes

$$d\sigma^{pA \rightarrow \eta' X} = \int dx_1 dx_2 d^2 p_t G^p(x_1, Q_f^2) G^A(x_2, Q_f^2, p_t) d\sigma^{gg \rightarrow \eta'} \quad (23)$$

where $G^A(x, Q_f^2, p_t^2) = G^A(x, Q^2) f(p_t^2)$ and $f(p_t^2)$ is a Gaussian (8) with width of Q_s^2 .

Substituting Eq. (12) and using the δ functions gives

$$\frac{d\sigma^{pA \rightarrow \eta' X}}{d^2 P_t dx_L} = \frac{\pi H_0^2}{64 x_E} x_1 G^p(x_1, Q_f^2) x_2 G^A(x_2, Q_f^2, P_t) \quad (24)$$

where $x_1 = M_{\eta'}^2/sx_-$ and $x_2 = x_-$ and P_t is the measured transverse momentum of the produced η' . Therefore, measuring the produced η' at different rapidities (x_L) and transverse momentum would determine the gluon distribution of nucleus at various x and scale $Q_f \sim M_{\eta'}$.

To get a feeling for the kinematics region where one can extract the nuclear gluon distribution function, let us set $P_t = 1$ GeV for RHIC. The range of accessible x_2 for the nucleus is now

$$3.3 \times 10^{-5} < x_2 < 0.007 \quad (\text{RHIC}) \quad (25)$$

which is still very small. For LHC, we have access to higher transverse moment. If we set $P_t = 5$ GeV. The range of x_2 in this case is

$$1.7 \times 10^{-7} < x_2 < 9.3 \times 10^{-4} \quad (\text{LHC}) \quad (26)$$

Even for this large P_t , the accessible x_2 range goes much beyond the currently accessible region.

Let us now consider the most general case when both the incoming proton and nucleus have intrinsic momenta. It is still expected that the intrinsic momentum of the proton should be less than that of a nucleus. In principle, we could also introduce a saturation scale for protons since at high enough energies (small x), the non-linearities of the gluonic fields which lead to the saturation scale would become important even in a proton. However, in this work, we would like to restrict ourselves to not too small values of x in a proton so that we can explore the very small x region in a nucleus. Therefore, we will ignore high gluon densities effects in a proton and take the average intrinsic momentum in the proton as determined in pp experiments.

In the case when both proton and nucleus have transverse momenta, the momenta of the incoming gluons become

$$q = (x_1\sqrt{s}/2 + q_t^2/2x_1\sqrt{s}, q_t, x_1\sqrt{s}/2 - q_t^2/2x_1\sqrt{s}) \quad (27)$$

and

$$p = (x_2\sqrt{s}/2 + p_t^2/2x_2\sqrt{s}, p_t, -x_2\sqrt{s}/2 + p_t^2/2x_2\sqrt{s}) \quad (28)$$

The differential cross section then can be written as

$$d\sigma^{pA \rightarrow \eta' X} = \int dx_1 dx_2 d^2 p_t d^2 q_t G^p(x_1, Q_f^2, q_t) G^A(x_2, Q_f^2, p_t) d\sigma^{gg \rightarrow \eta'} \quad (29)$$

which, upon using Eq. (12), becomes

$$\frac{d\sigma^{pA \rightarrow \eta' X}}{dx_L d^2 P_t} = \frac{\pi H_0^2}{64 x_E} \int d^2 p_t x_1 G^p(x_1, Q_f^2, q_t) x_2 G^A(x_2, Q_f^2, p_t) \frac{M^2}{|\hat{M}^2 - p_t^2 q_t^2 / \hat{M}^2|} \quad (30)$$

where $q_t = P_t - p_t$ and

$$\hat{M}^2(p_t, q_t) = \frac{1}{2} \left(M^2 + 2p_t \cdot q_t + \sqrt{(M^2 + 2p_t \cdot q_t)^2 - 4p_t^2 q_t^2} \right) \quad (31)$$

with

$$x_1 = \frac{\hat{M}^2 + q_t^2}{sx_-} \quad x_2 = \frac{x_- \hat{M}^2}{\hat{M}^2 + q_t^2}, \quad (32)$$

using $x_{\pm} = (x_E \pm x_L)/2$. The p_t integration can be performed numerically which would then directly relate the gluon distribution function in a nucleus $G^A(x, Q_f^2)$ at x and $Q_f^2 \sim M_{\eta'}^2$ to the measured rapidity and P_t of the produced η' .

However, since the η' production cross section in pA collisions is not experimentally known, we can conversely use the available parameterizations of the nuclear gluon distribution function to predict the η' production cross section in pA collisions, for example, in those planned at RHIC. In this work, we will take this approach and use two available parameterizations of the gluon distribution function in nuclei due to [11] and [12].

In Figure (1) we show the double differential cross section $\frac{d\sigma^{pA \rightarrow \eta'}}{dx_L d^2 P_t}$ as a function of η' transverse momentum at $x_L = 0.1$ for two different values of the intrinsic momentum (saturation scale) in the nucleus. As is seen, increasing the intrinsic

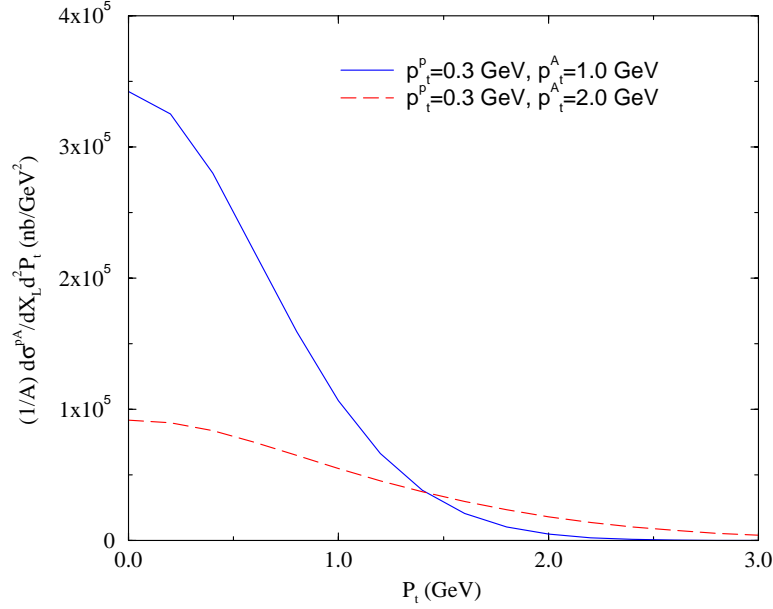


Figure 1: η' production cross section in pA at $x_L = 0.1$ and $\sqrt{s} = 200$ vs. η' transverse momentum P_t .

momentum reduces the differential cross section by a factor of 3 – 4. It should be noted that were we to plot our results vs. rapidity, the cross section would increase with increasing intrinsic momentum.

In Figure (2) we show the P_t integrated cross section vs. the η' longitudinal momentum ratio x_L . Again a decrease in the cross section is seen as we go to higher intrinsic momenta. In both Figures (1) and (2) BQV shadowing [12] is used.

In Figure (3) we show the ratio of η' production cross sections in pp and pA collisions for two representative values of the nuclear intrinsic momenta. As shown, this ratio is quite sensitive to the value of the intrinsic momenta. We have checked that the choice of parameterization of nuclear shadowing ([11] or [12]) makes very little difference.

Following the thermal model estimate, we expect that the total cross-section for η' production should be about 3–5% of π^0 cross-section. Among the decay mode of η' , the experimentally cleanest one is the $\eta' \rightarrow \gamma\gamma$ channel. This process has the branching ratio of about 2 %. Therefore, the branching ratio times the cross-section should be on the order of $A\sigma_{\pi^0}/1000 \sim 1$ mb. To measure this at RHIC, one will have to separate these photons from those coming from other sources. Nevertheless,

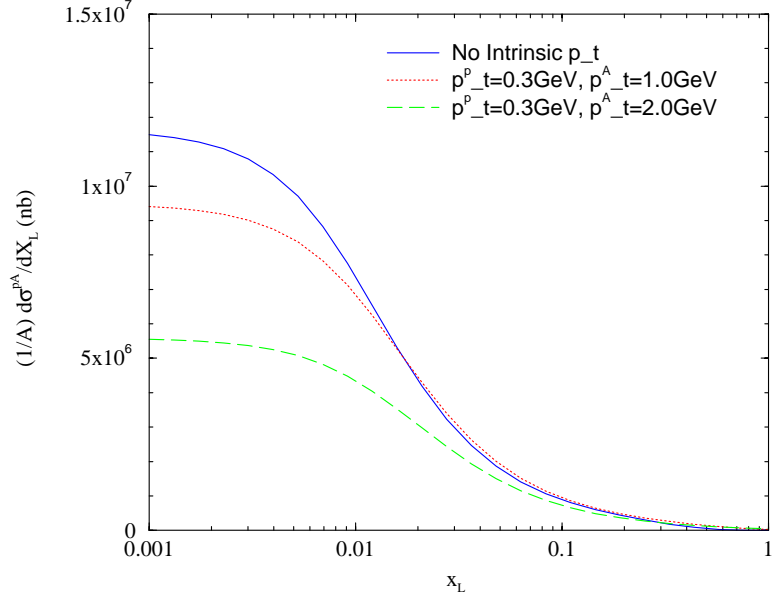


Figure 2: η' production cross section at $\sqrt{s} = 200$ vs. x_L .

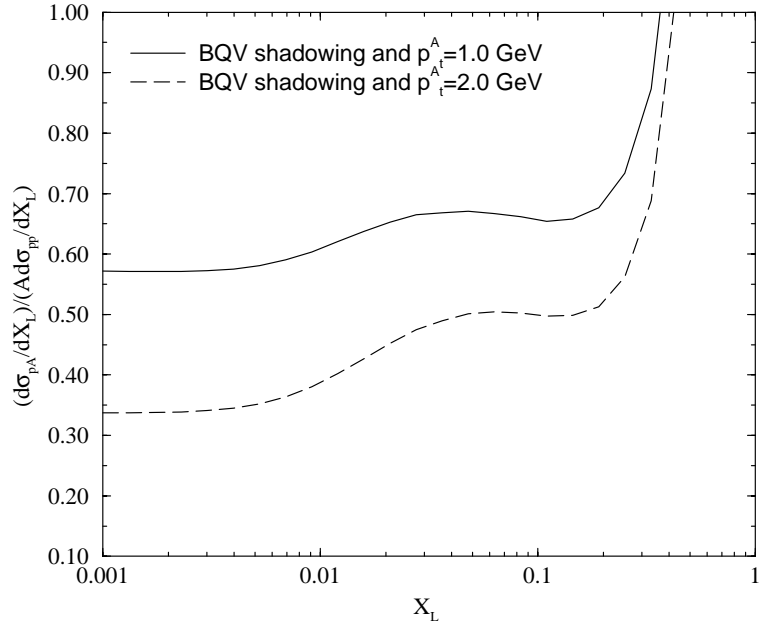


Figure 3: Ratio of pA to pp η' production cross sections at $\sqrt{s} = 200$.

both STAR and PHENIX detectors will be able to detect η 's. As a very rough estimate, PHENIX may be able to measure η 's in the transverse momentum range $1 < p_t < 5\text{GeV}$ and (pseudo)rapidity range -0.3 to 0.3 [39].

3 Conclusion

We have investigated the production of η' in pA collisions and its sensitivity to the intrinsic momenta (saturation scale) in nuclei. We have shown that experimental measurement of this cross section at RHIC would lead to determination of the gluon distribution function in nuclei in a much wider kinematic region accessible by any other process in the current experiments. Conversely, we have used the available parameterizations of the gluon distribution function in nuclei to predict the η' production cross section in pA collisions at RHIC.

There are several points which need to be better understood in order to make our calculation more accurate. First of all, we have included only the gluon fusion and ignored all other possible mechanisms of η' production. For example, it may be possible to produce η' through production of quarks and anti-quarks which would hadronize into a η' through a completely non-perturbative fragmentation function. The effect of this mechanism is hard to estimate since quark (or anti-quark) fragmentation into η' has not been measured.

We have also taken the η' mass to be a constant (958 MeV) since we don't expect to have a Quark Gluon Plasma produced in a pp or pA collision. One then would have had to investigate the temperature dependence of the anomaly and include the poorly understood temperature dependence of the η' mass. However, there is a recent study of high gluon density effects on instantons [40] which indicates the average instanton size shrinks as the saturation scale Q_s grows analogous to the finite temperature case. This would imply that η' would become lighter and its production cross section would increase at higher energies due to the rise of Q_s . Decreasing η' mass would reduce our $gg\eta'$ matrix element (11) and our η' production cross section. Therefore measuring η' production cross section at different energies, for example at RHIC would help clarify this point.

Also, we are using the collinear factorization for a process for which there is no proof even though one may naively expect it to hold in analogy to heavy quark production. Our factorization scale, $M_{\eta'}^2$ is not very high and our results are somewhat sensitive to the change in this scale. Therefore, we feel that our results are most reliable for ratio of pA to pp cross sections for η' production.

Acknowledgement

We would like to thank C. Gale, D. Kharzeev, L. McLerran, R. Venugopalan and W. Zajc for useful discussions. J.J-M. is supported in part by a LDRD from BSA and by U.S. Department of Energy under Contract No. DE-AC02-98CH10886. S.J. is supported in part by the Natural Sciences and Engineering Research Council of Canada and by le Fonds pour la Formation de Chercheurs et l'Aide à la Recherche du Québec.

References

- [1] G. 't Hooft, Phys. Rev. Lett. **37**, 8 (1976).
- [2] E. Witten, Nucl. Phys. B **156**, 269 (1979).
- [3] D. Atwood and A. Soni, Phys. Lett. B **405**, 150 (1997)
- [4] A. L. Kagan and A. A. Petrov, “ η' production in B decays: Standard model vs. new physics,” hep-ph/9707354.
- [5] T. Muta and M. Z. Yang, “QCD anomaly coupling for the $\eta'gg$ vertex in inclusive decay $B \rightarrow \eta'X$,” hep-ph/9902275.
- [6] S. Jeon, “Production of η' from thermal gluon fusion,” hep-ph/0107140.
- [7] A. M. Cooper-Sarkar, R. C. Devenish and A. De Roeck, Int. J. Mod. Phys. A **13**, 3385 (1998).
- [8] M. Arneodo, Phys. Rept. **240**, 301 (1994).
- [9] J. Jalilian-Marian and X. N. Wang, Phys. Rev. D **60**, 054016 (1999).
- [10] J. Jalilian-Marian and X. N. Wang, Phys. Rev. D **63**, 096001 (2001).
- [11] K. J. Eskola, V. J. Kolhinen and P. V. Ruuskanen, Nucl. Phys. B **535**, 351 (1998).
- [12] C. J. Benesh, J. Qiu and J. P. Vary, Phys. Rev. C **50**, 1015 (1994).
- [13] L. Apanasevich *et al.*, Phys. Rev. D **63**, 014009 (2001).
- [14] E. Laenen, G. Sterman and W. Vogelsang, Phys. Rev. D **63**, 114018 (2001).
- [15] G. Papp, P. Levai and G. Fai, Phys. Rev. C **61**, 021902 (2000).

- [16] L. D. McLerran and R. Venugopalan, Phys. Rev. D **49**, 2233 (1994).
- [17] L. D. McLerran and R. Venugopalan, Phys. Rev. D **49**, 3352 (1994).
- [18] L. D. McLerran and R. Venugopalan, Phys. Rev. D **59**, 094002 (1999).
- [19] Y. V. Kovchegov, Phys. Rev. D **55**, 5445 (1997).
- [20] Y. V. Kovchegov, Phys. Rev. D **54**, 5463 (1996).
- [21] A. D. Martin, R. G. Roberts, W. J. Stirling and R. S. Thorne, Eur. Phys. J. C **14**, 133 (2000).
- [22] M. R. Adams *et al.* [E665 Collaboration], Z. Phys. C **67**, 403 (1995).
- [23] P. Amaudruz *et al.* [New Muon Collaboration], Nucl. Phys. B **371**, 3 (1992).
- [24] A. H. Mueller and J. Qiu, Nucl. Phys. B **268**, 427 (1986).
- [25] L. V. Gribov, E. M. Levin and M. G. Ryskin, Phys. Rept. **100** (1983) 1.
- [26] A. Ayala, J. Jalilian-Marian, L. D. McLerran and R. Venugopalan, Phys. Rev. D **52**, 2935 (1995).
- [27] A. Ayala, J. Jalilian-Marian, L. D. McLerran and R. Venugopalan, Phys. Rev. D **53**, 458 (1996).
- [28] J. Jalilian-Marian, A. Kovner, L. D. McLerran and H. Weigert, Phys. Rev. D **55**, 5414 (1997).
- [29] Y. V. Kovchegov and A. H. Mueller, Nucl. Phys. B **529**, 451 (1998).
- [30] J. Jalilian-Marian, A. Kovner, A. Leonidov and H. Weigert, Nucl. Phys. B **504**, 415 (1997).
- [31] J. Jalilian-Marian, A. Kovner, A. Leonidov and H. Weigert, Phys. Rev. D **59**, 014014 (1999).
- [32] J. Jalilian-Marian, A. Kovner and H. Weigert, Phys. Rev. D **59**, 014015 (1999).
- [33] J. Jalilian-Marian, A. Kovner, A. Leonidov and H. Weigert, Phys. Rev. D **59**, 034007 (1999) [Erratum-ibid. D **59**, 099903 (1999)].
- [34] A. Kovner and J. G. Milhano, Phys. Rev. D **61**, 014012 (2000).
- [35] A. Kovner, J. G. Milhano and H. Weigert, Phys. Rev. D **62**, 114005 (2000).

- [36] E. Iancu, A. Leonidov and L. D. McLerran, Nucl. Phys. A **692**, 583 (2001).
- [37] E. Iancu, A. Leonidov and L. D. McLerran, Phys. Lett. B **510**, 133 (2001).
- [38] E. Ferreira, E. Iancu, A. Leonidov and L. McLerran, hep-ph/0109115.
- [39] W. Zajc, private communication.
- [40] D. E. Kharzeev, Y. V. Kovchegov and E. Levin, hep-ph/0106248.